Chinese Journal of Aeronautics, (2013),26(5): 1336–1345

Chinese Society of Aeronautics and Astronautics
& Beihang University

Chinese Journal of Aeronautics

cja@buaa.edu.cn
www.sciencedirect.com

Springback prediction of thick-walled high-strength titanium tube bending

Song Feifei [a], Yang He [a,*], Li Heng [a], Zhan Mei [a], Li Guangjun [b]

[a] State Key Laboratory of Solidification Processing, School of Materials Science and Engineering, Northwestern Polytechnical University, Xi'an 710072, China
[b] Chengdu Aircraft Industry (Group) Corporation Ltd., Chengdu 610092, China

Received 5 September 2012; revised 20 November 2012; accepted 10 January 2013
Available online 2 August 2013

KEYWORDS

Bending;
Finite element method;
High strength;
Numerical parameters;
Solid elements;
Springback;
Titanium alloys;
Tube

Abstract Significant springback occurs after tube rotary-draw-bending (RDB), especially for a high-strength Ti–3Al–2.5V tube (HSTT) due to its high ratio of yield strength to Young's modulus. The combination scheme of explicit and implicit is preferred to predict the springback. This simulation strategy includes several numerical parameters, such as element type, number of elements through thickness (N_{EL}), element size, etc. However, the influences of these parameters on springback prediction accuracy are not fully understood. Thus, taking the geometrical specification 9.525 mm × 0.508 mm of a HSTT as the objective, the effects of numerical parameters on prediction accuracy and computation efficiency of springback simulation of HSTT RDB are investigated. The simulated springback results are compared with experimental ones. The main results are: (1) solid and continuum-shell elements predict the experimental results well; (2) for C3D8R elements, N_{EL} of at least 3 is required to obtain reliable results and a relative error of 29% can occur as N_{EL} is varied in the range of 1–3; (3) specifying damping factor typically works well in Abaqus/Emplicit simulation of springback and the springback results are sensitive to the magnitude of damping factor. In addition, the explanations of the effect rules are given and a guideline is added.

1. Introduction

Owing to excellent characters like high strength-to-weight ratio, corrosion resistance, long life-span, etc., titanium alloy tubes have been widely used in hydraulic pneumatic, fuel or environment control systems for advanced aircraft and spacecraft as bleeding components.[1] The strength of stress-relieved Ti–3Al–2.5V tube reaches above 724 MPa,[2] which is so-called high-strength titanium alloy tube (HSTT). HSTT can satisfy higher requirements of specific applications in aircraft and spacecraft areas. Among many tube bending methods such as pure bending, push bending, and compression bending, rotary-draw-bending (RDB) has become an advanced and preferred technology in tube bending manufacture with high accuracy and efficiency. As shown in Fig. 1(a), to form a tube to a desired shape, combined operations are conducted by multiple dies including bending die, pressure die, clamp die, and

* Corresponding author. Tel.: +86 29 88495632.
E-mail addresses: songff060898@163.com (F. Song), yanghe@nwpu.edu.cn (H. Yang), liheng@nwpu.edu.cn (H. Li).

Peer review under responsibility of Editorial Committee of CJA.

1000-9361 © 2013 Production and hosting by Elsevier Ltd. on behalf of CSAA & BUAA. Open access under CC BY-NC-ND license.
http://dx.doi.org/10.1016/j.cja.2013.07.039

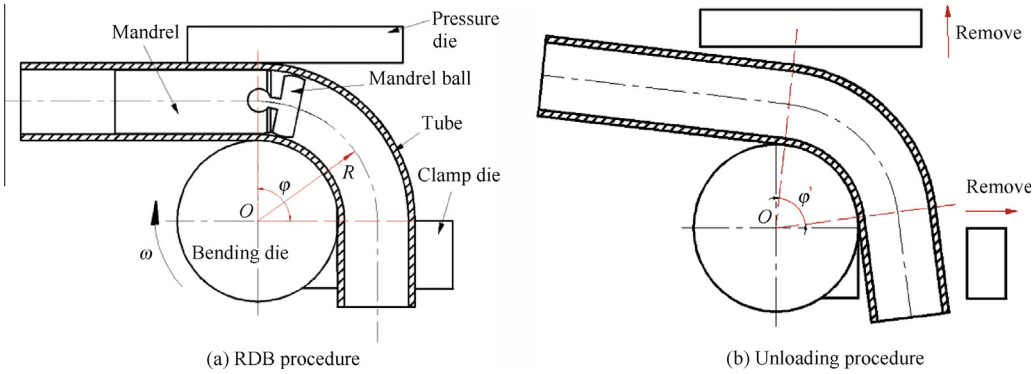

Fig. 1 Schematics of the RDB and unloading procedures.

mandrel. Significant springback of HSTTs happens after the unloading procedure (as shown in Fig. 1(b)) due to its high ratio of yield strength to Yong's modulus. The significant springback affects both geometrical and shape accuracy, which directly determines the connection and sealing performance of tubes with other parts as well as the internal structure compact.[3,4] Thus, the springback evaluation of titanium tube bending becomes an urgent problem to be solved for improving the overall performance of advanced aircraft and spacecraft.

Over the past few years, there have been a lot of studies about springback simulation of sheet metal forming processes such as deep drawing and U-bending. For numerical simulation of sheet metal forming processes, an appropriate constitutive model which properly describes stress–strain responses of materials is needed. Yoshida and Uemori[5] presented a constitutive modeling of large-strain cyclic plasticity which described both deformation and texture-induced anisotropies of materials. Lee et al.[6] proposed an analytical model for asymmetric elasto-plastic bending under tension followed by elastic unloading in order to evaluate the bending moment. For the verification purpose, the springback of AZ31B magnesium alloy sheets was measured using an unconstrained cylindrical bending test of Numisheet and a 2D draw bend test.[7] Lee et al. [8] described the implementation of a proposed constitutive model into an elastic–plastic finite element method. A new stress update algorithm was developed to efficiently integrate the stress state during plastic deformation. The above researchers made great contributions to the development of elasto-plastic constitutive modeling, especially in case of large-strain cyclic plasticity.

However, springback result simulated by the FE model is sensitive not only to many physical parameters including material constitutive model, geometric and processing parameters, but also to some numerical schemes or parameters such as element type, number of element through thickness (N_{EL}), element size, etc. Ortiz and Popov[9] carried out an analysis of accuracy and stability of algorithms for the integration of elasto-plastic constitutive relations. Lee et al.[10] considered two stress integration algorithms based on the closest point projection method and the general convex cutting plane method for the integration of the new distortional hardening model recently proposed by Barlat et al.[11] Lee and Yang[12] found that blank element size as well as number of corner elements were the most significant factors influencing springback in sheet metal forming processes, and obtained the optimal element sizes for blank and tool corners. Li et al.[13,14] carried out a series of simulations of the draw/bend test over a typical range of process variables for three typical sheet alloys. For the choices of numerical parameters, up to 51 integration points (IPs) through sheet thickness were required for accuracy within 1%, and improvements were also needed in the number of elements in contact with the tools. This study also revealed that 3D shell and non-linear solid elements were preferred for springback. Papeleux and Ponthot[15] investigated the influence on springback of a time integration algorithm, and found that the results were slightly different whether an implicit or explicit scheme was used, but there was main difference in the CPU cost. Xu et al.[16] used an explicit method in springback simulation for sheet metal forming, and found that number of integration points and blank sheet element size were sensitive in springback simulation.

Up to now, the research work on factors influencing springback of tube bending has been focused mainly on physical parameters, while the numerical parameters' effects are less considered and the relevant literature is scant. Jiang et al.[17,18] established a three-dimensional (3D) FE model for RDB of a middle-strength titanium alloy tube considering both bending and springback, but in their work only single/double precision and mass scaling factor were fully investigated while the choices of other numerical parameters were not mentioned too much.

Since the bending process involves extreme nonlinearities and contact interaction while the springback process involves only mild nonlinearities and no contact, a combination of explicit forming and implicit springback simulations has been popular.[12,17–19] This simulation strategy includes a couple of numerical parameters, such as element type, number of elements through thickness, element size, mass scaling factor, automatic stabilization method, etc. Presently, the accuracy and reliability of FE analyses do not yet satisfy the industrial requirements of tube bending. The influence rules of all these numerical parameters on springback prediction should be thoroughly investigated and clarified to improve the springback prediction accuracy of HSTT RDB as well as precise bending deformation. Hence, in this paper taking the geometrical specification $9.525\,\text{mm} \times 0.508\,\text{mm}$ of a HSTT as the objective, the effects of numerical parameters in both explicit and implicit algorithms on the prediction accuracy and computation efficiency of springback prediction of HSTT bending are investigated. The simulated springback results are compared

with experimental ones. Finally, the explanations of the effect rules are given and a selection guide is presented.

2. Experimental procedure of HSTT RDB

Prior to the RDB process, a mandrel is properly positioned in a hollow tube, and then the tube is clamped against a bending die by a clamp die and a pressure die. Since the diameter-to-thickness (D/t) ratio of the HSTT is 18.75, which is considered thick-walled ($D/t < 20$), wrinkling is unlikely to occur, thus the wiper die is removed considering to minimize the manufacture costs.

When bending begins, the tube is drawn by the clamp die and the bending die, and rotates along the groove of the bending die to a desired bending radius and bending angle, as shown in Fig. 1(a). The mandrel is withdrawn after bending, and then both the clamp die and the pressure die are removed, as shown in Fig. 1(b). The forming parameters in experiments and FE models are listed in Table 1.

During the process, IRMCO GEL 980-301 is used as the lubricant between the tube and the dies, and the friction coefficients obtained by a twist-compression test[20] for different contact interfaces are listed in Table 2. Experiments are conducted on a computer-numerical-control (CNC) tube bender BLM DYNAMO-E LR150. The springback results are obtained by a non-contact laser probe with relatively high accuracy. Sample tubes having different bending angles are shown in Fig. 2.

Table 1 Forming parameters in experiments and FE models.

Items	Values
Bending radius R (mm)	28.575
Bending speed ω (rad/s)	1.16
Pushing speed of pressure die V_p (mm/s)	38.45
Bending angle φ (°)	30, 101, 120, 166
Mandrel diameter d (mm)	8.35
Mandrel extension length e (mm)	0
Number of balls	1
Ball diameter (mm)	8.32
Thickness of balls (mm)	3.5
Length of clamp die (mm)	28.6
Length of pressure die (mm)	132.7

Table 2 Friction conditions at various contact interfaces.

Contact interface	Tool material	Friction coefficients
Tube/clamp die	Cr18MoV	Rough
Tube/pressure die	Cr18MoV	0.25
Tube/bending die	Cr18MoV	0.1
Tube/mandrel	Al–bronze	0.05
Tube/mandrel ball	Al–bronze	0.05

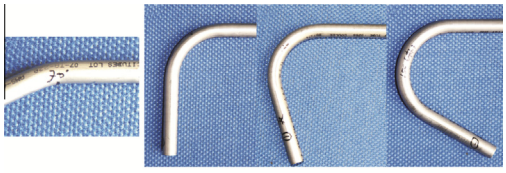

(a) φ=30° (b) φ=101° (c) φ=120° (d) φ=166°

Fig. 2 Sample tubes having different bending angles.

3. FE model description

3.1. Material property

Mechanical properties of the HSTT are measured by a uniaxial tension test of a complete tube sample (SAE AMS 4944/F) according to GB/T 228-2002. The test is carried out on a longitudinal extensometer YSJ-50/25-ZC with a gauge of 50 mm and a range of 25 mm, and at the same time, a transverse extensometer is used to achieve the Lankford's r-value considering the plastic anisotropy. The true stress–strain curves of the tube material and a specimen are shown in Fig. 3. The exponent hardening law as $\bar{\sigma} = K(a + \bar{\varepsilon})^n$ is used to calibrate the stress–strain curves. The determined material properties are presented in Table 3. On one hand, the anisotropy in the plane is approximately eliminated after stress relief annealing, and almost only increases strength reserved in the thickness direction of the tube. On the other hand, the maximum strain during the tube bending process is less than 0.2. In this case, the Bauschinger effect can be ignored. Therefore, the so-called transverse anisotropy can be modeled by the Hill48 yield criterion appropriately. In the code Abaqus, the criterion's parameters are linked to the yield stress ratio R_{ij} and subsequently to the Lankford's r-value so that

$$R_{11} = \sqrt{\frac{r+1}{2}} \tag{1}$$

$$R_{22} = R_{33} = R_{12} = R_{13} = R_{23} = 1 \tag{2}$$

where R_{ij} is the yield stress ratio and r is the Lankford's value.

Herein, the Lankford's r is 1.508, and then R_{11} is calculated as 1.1198. Subscript '1' denotes the thickness direction, '2' the hoop direction, and '3' the tangential to the bend direction in

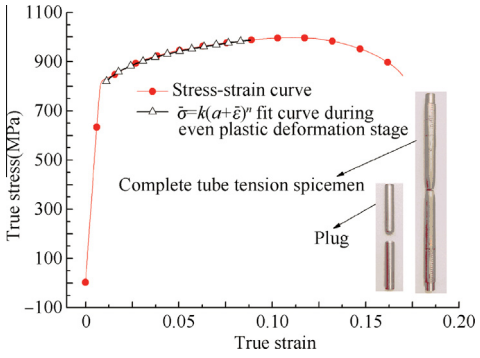

Fig. 3 Stress–strain curve and fitting results.

Table 3 Mechanical properties of the HS Ti–3Al–2.5V tube.

Items	Value
Young's modulus E (GPa)	104.8572
Fracture elongation (%)	18.75
Initial yield stress (MPa)	817.50
Ultimate strength (MPa)	905.00
Strength coefficient K (MPa)	1239.5500
Hardening exponent n	0.0914
Material constant a	−0.0004
Lankford's r	1.5080

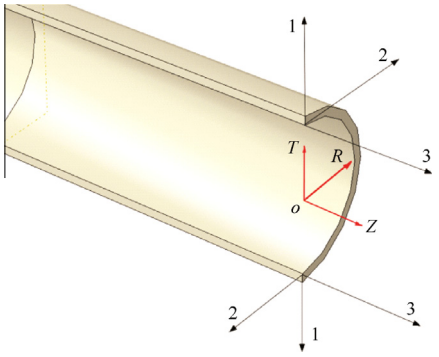

Fig. 4 Material direction of the half tube model.

which the uniaxial tension test is performed. Fig. 4 shows the material direction of the half tube in the FE model.

3.2. FE modeling

In order to improve computing efficiency, half tube and die models are adopted due to the symmetrical forming conditions, as showed in Fig. 5. Moreover, the tube is divided into two portions axially: the bending portion and the straight portion. In the bending portion, the mesh size is smaller than that in the straight portion. The dies are modeled as rigid bodies using 4-node 3D bilinear quadrilateral rigid element R3D4 to describe contact geometrical curved faces. The springback happens after removing the dies, and the contact release method[13] is adopted to simulate the springback process. The coulomb's friction model is chosen to represent the friction behaviors between the tube and various dies.

4. Results and discussion

4.1. Influence of the element type

Due to the specific geometrical character of the tube and the complex applied loadings through the RDB, the FE models are established in three dimensions, and 3D elements are employed. Generally, a solid element is employed when D/t is below 15, otherwise a shell element is used. The D/t of the HSTT specification is 18.75, which is close to the critical value of 15. Thus, both shell elements and solid elements are considered. Besides, a continuum shell element is similar to a shell element but discretizes an entire 3D body. Therefore, conventional shell elements, continuum shell elements, and hexahedral solid elements are analyzed. S4R (4-node quadratic thick shell) and C3D8R (8-node linear brick) are more attractive in FEM because they are robust and suitable for a wide range of applications under the condition of being finely meshed. Moreover, they can achieve the minimum cost when compared with some quadratic elements such as C3D20 or C3D20R (C3D20 and C3D20R are not available in Abaqus/Explicit, and thus these two types of elements cannot be used in forming simulations[21]). Finally, simulations are carried out using S4R, C3D8R, and SC8R elements respectively.

Sufficient fine meshes must be used in places of high stress gradients, which are suggested according to the theory of FE analysis to reduce errors due to discretization. Hence, mesh size 0.5 mm is used alone Direction 3, that is, an angle of 1° per element over the bending portion is adopted initially. Considering the curvature of the tube section, mesh size 0.5 mm is used along Direction 2, that is, an angle of 6.7° per element is used to smooth the section curvature, as shown in Fig. 6. Theoretically, in order to avoid the hourglassing, four elements should be used through the thickness,[21,22] and "enhanced" hourglass control is applied. Therefore, C3D8R and SC8R calculations use a mesh size of 0.5×0.5 (Direction $3 \times$ Direction 2, mm, the default direction if not mentioned again below) in the bending portion and four elements through the thickness. Meanwhile, S4R calculations use a mesh size of 0.5×0.5 and 4 Gauss IPs are used in the shell section property. To eliminate the impacts of the number of IPs on the comparison results, 9 IPs of shell elements are added to calculations.

Calculation results are compared with experimental ones, as shown in Fig. 7(a). It shows that using the same number of IPs and mesh size, C3D8R and SC8R predict the experimental results well while S4R shows discrepancies even in a fine mesh. In addition, increasing the number of IPs of shell elements does not improve the simulation accuracy. It can be seen from Fig. 7(b) and (c) that the magnitudes of Mises stress at both extrados and intrados of the tube for S4R elements are significantly lower than those for C3D8R and SC8R elements, and thus the springback moment of S4R elements is lower than those of C3D8R and SC8R elements, which causes the above results. In the view of total CPU time, as showed in Fig. 7(d), SC8R takes up the most time, followed by C3D8R. S4R spends the least time which is less than half of that for C3D8R. As a result, to balance between efficiency and accuracy of springback prediction, the 8-node linear brick,

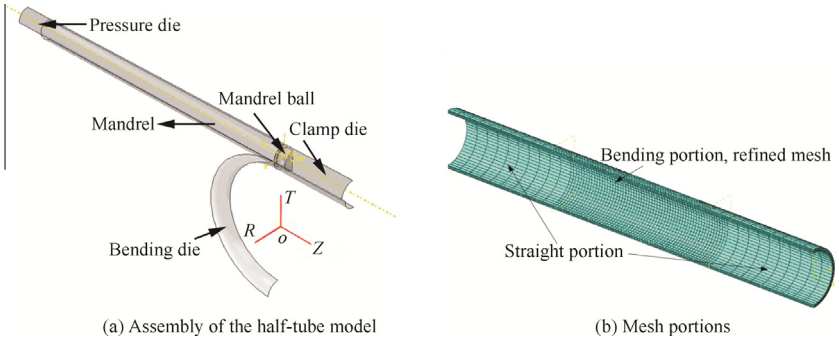

(a) Assembly of the half-tube model (b) Mesh portions

Fig. 5 Schematics of assembly of the half-tube model and mesh portions.

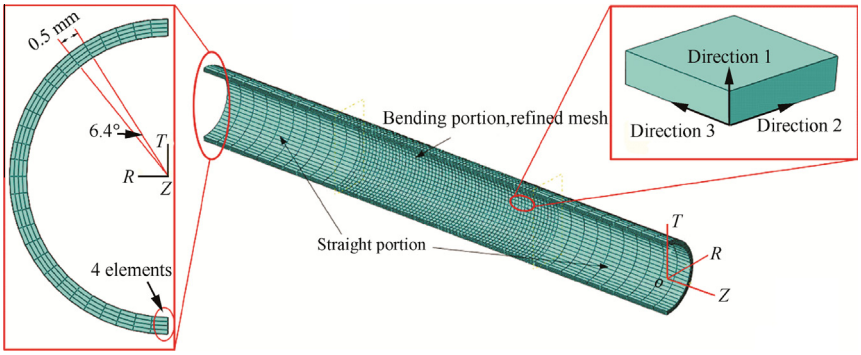

Fig. 6 Initial mesh size and default direction.

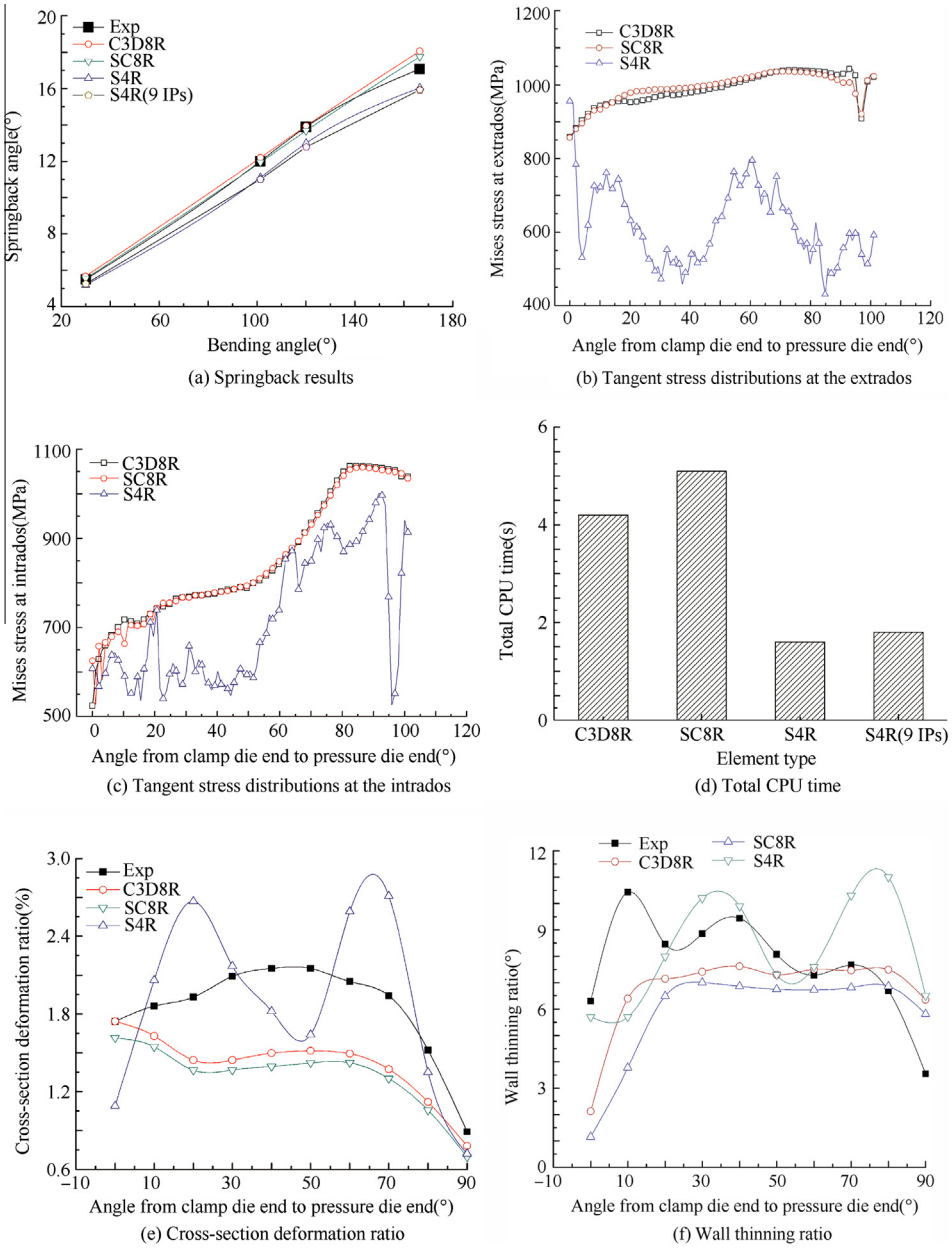

Fig. 7 Comparison results of the bending process for different element types (*Processor: 2.33 GHz, RAM: 4 GB).

reduced-integration, solid element (C3D8R) with hourglass control is recommended.

Though shell elements are too soft in springback prediction, they may show advantages of cost-effective in other industrial applications. It is found that, shell elements can reach reasonable results such as cross-section deformation ratio and wall thinning ratio, as shown in Fig. 7(e) and (f). Note that for the numerical results, the discrepancies are mainly caused by the idealized contact conditions used in the FE models such as unchanged friction conditions and stable tooling movements.

4.2. Influence of the number of elements through thickness (N_{EL})

Once the element type has been evaluated and selected, all simulations reported in next section make use of the finding results above. Since a solid element C3D8R has a linear shape function, there is only one integration point standing at the center of the 8-node brick, i.e., an element represents an integration point. In order to investigate the influence of N_{EL} on the accuracy of the simulation results, various simulations have been performed respectively with 1, 2, 3, 4, 5, 6, and 9 elements through the 0.508 mm thickness. The mesh sizes in Direction 3 and Direction 2 are still remained at 0.5 mm.

The relative error for evaluating the accuracy of prediction results is described as Eq. (3). Fig. 8(a) shows that with the increase of N_{EL}, the springback results of different bending angles are tending toward stability. It can be seen from Fig. 8(b) that N_{EL} needs to be at least 3 for accuracy within 5%. Note that the relative error is about 6.3% when the bending angle is 166°. It may be caused by errors of idealized contact conditions. For a bending angle of 30°, a relative error of 29% can occur as N_{EL} is varied in the range of 1–3. It also indicates that when N_{EL} is more than 3, there are no obvious improvements on simulation accuracy by way of increasing N_{EL} only. In the view of computation time, more N_{EL} spends much more time. Therefore, N_{EL} of at least 3 is requested to obtain a reliable result whilst greatly decrease the computation time. The results are dramatically different from those previously recommended[13] for forming simulations. That is the reason why the previous findings cannot be directly applied in HSTT RDB simulations.

$$\text{Error} = \frac{V_{FE} - V_{Exp.}}{V_{Exp.}} \times 100\% \tag{3}$$

4.3. Influence of mesh size

The springback is the result of elastic strain releasing after bending, which is directly influenced by element size especially in the bending portion. For the hollow cylinder charactoristic of the tube, not only the mesh size in Direction 3, but also in Direction 2 need to be considered. Since Direction 3 is the most critical stress/strain direction in tube bending, mesh size in Direction 3 is analyzed firstly. In the bending portion, mesh sizes of 0.3, 0.5, 0.7, 1, 2, 3, and 4 mm are used respectively in simulations of the forming process. The mesh size in Direction 2 is still 0.5 mm, and N_{EL} of 3 is adopted. It can be seen in Fig. 9(a) that the springback angles slightly increase with the minishing of the mesh size in Direction 3. Fig. 9(b) indicates that the maximum mesh size in Direction 3 is 1 mm for accuracy whithin 6%, which is about an angle of 2° per element in the turning circle.

Then the mesh size in Direction 2 is analyzed sequently. As can be seen from Fig. 10(a), the springback results are tending toward stability with the minishing of the mesh size in Direction 2. Fig. 10(b) indicates that the maximum mesh size in Direction 2 is 0.5 mm for accuracy whithin 6%, which is about an angle of 6.4° per element in the tube hoop direction.

In conclusion, in order to obtain the balance between simulation accuracy and efficiency, an angle of 2° per element in the turning circle, an angle of 6.4° per element in the tube hoop direction, and 3 elements through thickness are recommended.

4.4. Influence of mass scaling actor (MSF)

Tube bending can be regarded as a quasi-static process. There are two approaches to obtain economical quasi-static solutions with an explicit dynamics solver. One is increasing load rates, and the other is applying MSF. Increasing load rates is meaningless due to the rate-insensitive tube material. Hence, applying MSF is chosen to achieve this goal.

The greater MSF is used. the more efficient. Nevertheless, overlarge MSF may generate incorrect results owing to bring in excessive kenitc effect. Therefore, MSF of 40000, 10000, 5000, 1000, 500, 100, and 1 are used individually to study the effects of MSF on springback prediction efficiency and accuracy. It can be seen from Fig. 11(a) that the computation time sharply increases with the decrease of MSF. For MSF of 1, the estimated computation time is about 300 days. However, the simulated results are almost the same except when MSF is

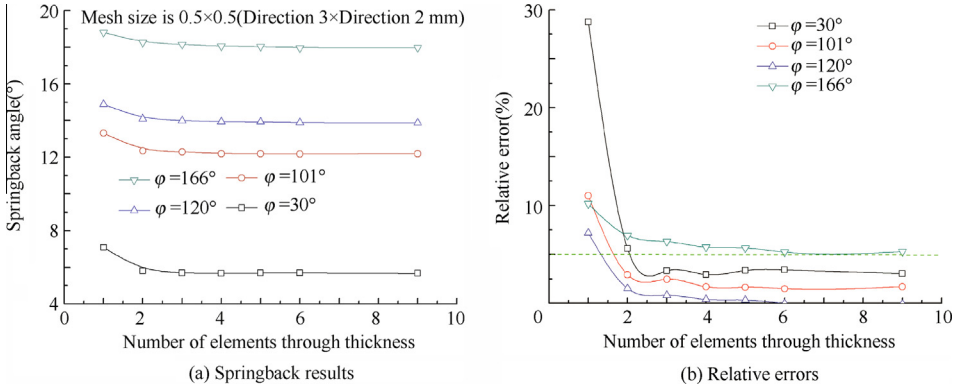

Fig. 8 Comparison results of the bending process for different N_{EL}.

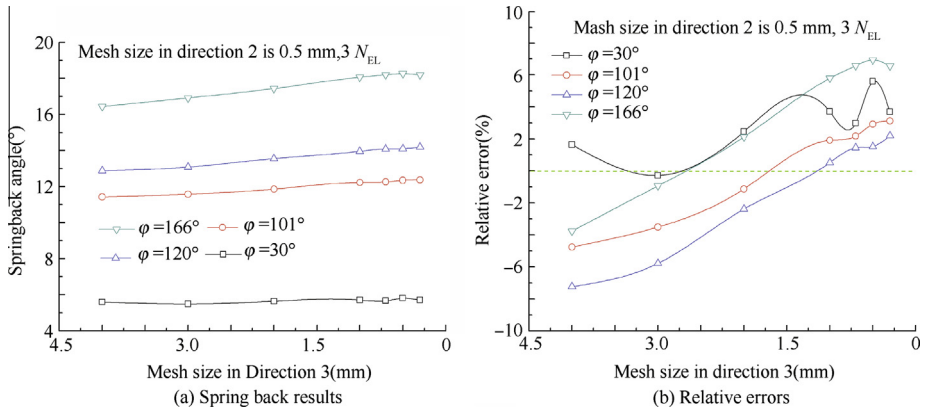

Fig. 9 Comparison results for different mesh sizes in Direction 3.

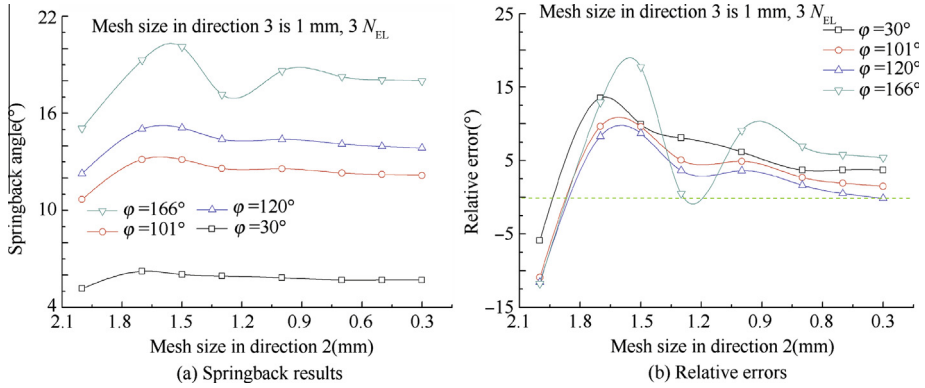

Fig. 10 Comparison results for different mesh sizes in Direction 2.

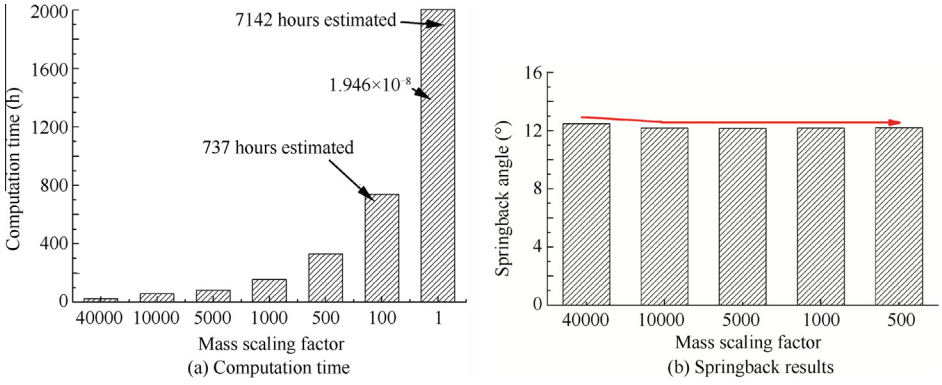

Fig. 11 Comparison results for different MSFs.

40000. By comprehensive considering, it is suitable when MSF is 10000 to obtain the tradeoff between computation accuracy and efficiency.

4.5. Convergence control in Abaqus/Standard

The HSTT springback problem may become unstable because of its severe nonlinearity. Therefore, Abaqus/Standard offers a set of automatic stabilization mechanisms to handle such a problem. After analyzing the numerical parameters in the explicit forming stage, the convergence control in static implicit simulation of springback should be investigated. An improper set of control parameters in Abaqus/Standard, such as automatic stabilization methods, initial increment size and precision set may result in incorrect results, even not convergence.

In Abaqus/Standard, there are three automatic stabilization schemes: specify dissipated energy fraction (Scheme 1), specify damping factor (DF) (Scheme 2), and use DF from previous general step (Scheme 3). Herein, these three methods are used respectively and the results are compared with experimental

ones. The default accuracy tolerance is 0.05, and the initial increment size is 0.001. It can be seen in Table 4 that the specify DF scheme typically works well to subside instabilities and to eliminate rigid body modes without having a major effect on the solution, which is in line with Abaqus documentation[21]. It can be seen from Jobs 4 and 5 that the precision set does not greatly affect the results. Therefore, it is preferable to specify DF rather than using other two schemes to obtain reliable springback results, and single precision is adopted in subsequent simulations.

However, the effect rules of above parameters on springback results are not understood. In practice, it is a time-consuming procedure to identify proper values of above parameters. To improve the efficiency, the effect rules of aforementioned parameters on simulation results should be addressed. Thus, series of simulations are conducted.

It can be seen from Jobs 2, 5, and 10 in Table 5 that the springback result decreases with the increase of DF. A decrease of 5.14° occurs when DF increases 1000 times. Comparing Jobs 1 and 2, or 4 and 5, or 9 and 10, it shows that setting the accuracy tolerance to 0 is good to converge and decreases computation time. It can also be seen from Jobs 5, 6, 7, and 8 that the initial increment size does not have a significant influence on simulation results, while magnifying initial increment size can greatly decrease computation time.

4.6. Discussion and guidelines

According to the above results, it can be addressed that solid elements are more proper for thick-walled tube springback prediction. There are many contact pairs in the tube bending process. The solid elements employ two-sided contact taking thickness changes into account, and reflect the stress/strain more precisely, that's why solid elements are more accurate in contact modeling than shell elements.

The linear reduced-integration elements (C3D8R) tend to be too flexible because they suffer from their own numerical problem called hourglassing.[21] In coarse meshes, the zero-energy mode can propagete through the meshs, producing meaningless results. Therefore, for C3D8R elements, N_{EL} of at least 3 is required to obtain reliable results. A relative error of 29% can occur as N_{EL} is varied in the range of 1–3.

An artificial stiffness is introduced to limit the propagation of the hourglass mode. This stiffness is more effective at limiting the hourglass mode when more elements are used in the model, which means that linear reduced-integration elements can give acceptable results as long as a reasonably fine mesh is used. That's the reason why springback results are tending towards stability with the minishing of mesh size.

In quasi-static analysis, there are a few smaller meshes which control the steady time increment of the whole model. Generally speaking, applying MSF can increase the size of the stable time increment, resulting in less computation time. However, overlarge MSF may introduce excessive kinetic energy (as shown in Fig. 12), which could generate large inertia forces. The inertia forces should be remained insignificantly in the quasi-static process. The principle to find a proper MSF is to increase MSF until the same results have been achieved.

For convergence control in Abaqus/Standard, obtaining an appropriate method, as well as the values of the paremeters, is a manual process requiring trials and errors until a converged

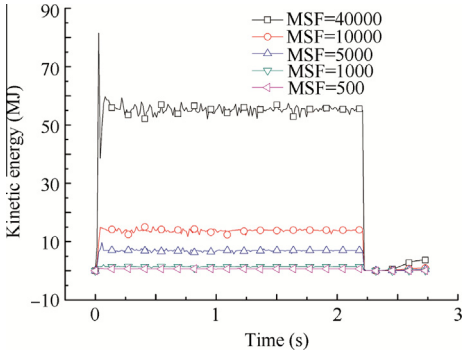

Fig. 12 Kinetic energy history with different mass scaling factors.

Table 4 Comparison results of influences of three automatic stabilization schemes on simulation accuracy and efficiency.

Job No.	Scheme	Value	Accuracy tolerance	Initial increment size	Precision set	Relative error (%)	Total CPU time (s)
1	1	0.0002	0.05	0.001	Single	Failed	
2	1	0.002	0.05	0.001	Single	Failed	
3	1	0.002	0	0.001	Single	≈100	796.5
4	2	0.0002	0.05	0.001	Single	2.90	710.6
5	2	0.0002	0.05	0.001	Double	2.90	689.9
6	3		0.05	0.001	Single	Failed	

Table 5 Comparison results of influences of different convergence parameters on simulation accuracy and efficiency.

Job No.	DF	Accuracy tolerance	Initial increment size	Simulation result (°)	Relative error (%)	Total CPU time (s)
1	0.0002	0.05	0.001	12.373	2.90	711
2	0.0002	0	0.001	13.370	11.19	607
3	0.002	0.05	0.1	12.377	2.94	532
4	0.02	0.05	0.001	12.361	2.80	1897
5	0.02	0	0.001	11.948	−0.63	709
6	0.02	0	0.01	11.950	−0.62	525
7	0.02	0	0.1	11.951	−0.61	363
8	0.02	0	1	11.950	−0.62	226
9	0.2	0.05	0.001	Failed		
10	0.2	0	0.001	8.233	−31.53	824

Table 6 Guidelines for thick-walled HSTT bending FE modeling.

Items	Recommended range
Explicit bending process	
Element type	Solid element (C3D8R or SC8R)
Number of element through thickness	At least 3
Element size	Maximum mesh size is: (a) An angle of 2° per element in turning circle; (b) An angle of 6.4° per element in tube hoop direction
Mass scaling factor	⩽10000
Implicit springback process	
Automatic stabilization method	Specify damping factor
Damping factor	About 0.02
Accuracy tolerance	About 0
Initial increment size	About 1

solution is achieved and the simulated results are close to experimental ones.

The explanations of how other numerical parameters are set in Abaqus/Standard are sophisticated and involve certain knowledge of equilibrium configuration. Thus, it is impossible to deal with them exhaustively in the limited space of this paper.

In order to provide some practical information for other researchers or manufacturers to quickly establish reliable and robust models, here are the guidelines (as shown in Table 6) for numerical parameters in thick-walled HSTT bending springback prediction modeling upon the Abaqus platform.

5. Conclusions

(1) Utilizing the same number of integration points through thickness, C3D8R and SC8R elements predict experimental results well while S4R elements show discrepancies even increasing the number of integration points. In addition, C3D8R elements spend less computation time compared with SC8R elements.

(2) The relative error can reach to 29% with coarse meshes. Therefore, the maximum mesh size for accuracy within 6% of C3D8R elements is: an angle of 2° per element in the turning circle versus 5°–10° recommended[14,22] and an angle of 6.4° per element in the tube hoop direction. At least 3 elements through thickness are required to obtain reliable results.

(3) The mass scaling factor should be chosen carefully to avoid bringing excessive kinetic energy. In Abaqus/Implicit springback, it is preferable to specify the damping factor rather than using the other two schemes to obtain reliable springback results. On the condition of convergence, the springback result decreases with the increase of damping factor. Moreover, the change of initial increment size does not affect the springback results. However, magnifying initial increment size can greatly decrease computation time.

Acknowledgements

The authors would like to thank the National Natural Science Foundation of China (No. 51275415), Program for New Century Excellent Talents in University, the fund of the State Key Laboratory of Solidification Processing in NWPU, Natural Science Basic Research Plan in Shaanxi Province (No. 2011JQ6004), and the 111 Project (No. B08040) for the support given to this research.

References

1. Boyer RR. An overview on the use of titanium in the aerospace industry. *Mater Sci Eng A* 1996;**213**(1–2):103–14.
2. AMS 4945E. Titanium alloy tubing, seamless, hydraulic 3Al–2.5V, controlled contractile strain ratio cold worked, stress relieved. Available from: http://www.standardsstore.org/RecordDetail.aspx?sku=SAE+AMS+4945E-2011+(SAE+AMS4945E-2011).
3. Yang H, Li H, Zhang Z, Zhan M, Liu J, Li GJ. Advances and trends on tube bending forming technologies. *Chin J Aeronaut* 2012;**25**(1):1–12.
4. Zhang S, Wu JJ. Spring-back prediction of non-planar tube bending. *Acta Aeronaut Astronaut Sin* 2011;**32**(5):953–60 [Chinese].
5. Yoshida F, Uemori T. A model of large-strain cyclic plasticity and its application to springback simulation. *Int J Mech Sci* 2003;**45**(10):1687–702.
6. Lee MG, Kim JH, Chung K, Kim SJ, Wagoner RH, Kim HY. Analytical springback model for lightweight hexagonal close-packed sheet metal. *Int J Plast* 2009;**25**(3):399–419.
7. Lee MG, Kim SJ, Wagoner RH, Chung K, Kim HY. Constitutive modeling for anisotropic/asymmetric hardening behavior of magnesium alloy sheet: application to sheet springback. *Int J Plast* 2009;**25**(1):70–104.
8. Lee JW, Lee MG, Barlat F. Finite element modeling using homogeneous anisotropic hardening and application to springback prediction. *Int J Plast* 2012;**29**:13–41.
9. Ortiz M, Popov EP. Accuracy and stability of integration algorithms for elasto-plastic constitutive relations. *Int J Numer Methods Eng* 1985;**21**:1561–76.
10. Lee JW, Lee MG, Barlat F, Kim JH. Stress integration schemes for novel homogeneous anisotropic hardening model. *Comput Methods Appl Mech Eng* 2012;**247–248**:73–92.
11. Barlat F, Gracio JJ, Lee MG, Rauch EF, Vincze G. An alternative to kinematic hardening in classical plasticity. *Int J Plast* 2011;**27**(9):1309–27.
12. Lee SW, Yang Y. An assessment of numerical parameters influencing springback in explicit finite element analysis of sheet metal forming process. *J Mater Process Technol* 1998;**80**:60–7.
13. Li KP, Geng L, Wagoner RH. Simulation of springback: choice of element. In: *Proceedings of the 6th ICTP*; 1999. p. 19–24.
14. Li KP, Carden WP, Wagoner RH. Simulation of springback. *Int J Mech Sci* 2002;**44**(1):103–22.
15. Papeleux L, Ponthot JP. Finite element simulation of springback in sheet metal forming. *J Mater Process Technol* 2002;**125**:758–91.
16. Xu WL, Ma CH, Li CH, Feng WJ. Sensitive factors in springback simulation for sheet metal forming. *J Mater Process Technol* 2004;**151**(1):217–22.
17. Jiang ZQ, Yang H, Zhan M, Yue YB, Liu J, Xu XD, et al. Establishment of a 3D FE model for the bending of a titanium alloy tube. *Int J Mech Sci* 2010;**52**(9):1115–24.
18. Jiang ZQ, Zhan M, Yang H, Xu XD, Li GJ. Deformation behavior of medium-strength TA18 high-pressure tubes during NC bending with different bending radii. *Chin J Aeronaut* 2011;**24**(5):657–64.
19. Sozen L, Guler MA, Bekar D, Acar E. Investigation and prediction of springback in rotary-draw-tube bending process using finite element method. In: *Proceedings of the Institution of Mechanical Engineers, Part C: Int J Mech Eng Sci*; 2012 March 2; 2012. p. 1–15.

20. Yang H, Li H, Zhan M. Friction role in bending behaviors of thin-walled tube in rotary-draw-bending under small radii. *J Mater Process Technol* 2010;**210**(15):2273–84.
21. Abaqus Inc. Abaqus analysis user's manual. Abaqus Inc.; 2004.
22. Meinders T, Burchitz IA, Bonte MHA, Lingbeek RA. Numerical product design: Springback prediction, compensation and optimization. *Int J Mach Tools Manuf* 2008;**48**(5):499–514.

Song Feifei is a postgraduate and received his B.S. degree in Materials Processing Engineering from Northwestern Polytechnical University in 2010. His main research focuses on springback of titanium alloy tubes.

Li Heng received his B.S., M.S., and Ph.D. degrees from Northwestern Polytechnical University. His main research interest lies in precise forming for large-scale complex/thin-walled lightweight components via multi-scale modeling and simulation.

Yang He is the "Cheung Kong" chair professor, Ph.D. His main research interests lie in advanced plastic forming and multi-scale modeling and simulation.